

Electronic supplementary information

Supplementary protocols

Text S1

Materials. Potassium dihydrogen phosphate (KH₂PO₄, 99.5%), methanol (CH₃OH, 99.5%), Tween 20 (≥40.0%), ammonium molybdate tetrahydrate ((NH₄)₆Mo₇O₂₄·4H₂O, >99%), zirconium tetrachloride (ZrCl₄, 98%) and ammonium metavanadate (NH₄VO₃, 99%) were purchased from RHAWN Reagents, IncShanghai, China. N, N-dimethylformamide (DMF, C₃H₇NO, 99.5%) and nitric acid (HNO₃, 98%) were purchased from Aladdin reagent company (Shanghai, China). Others were purchased from Cologne Chemicals Deionized (Chengdu, China). DI water (<18.2 MΩ·cm) was used throughout the experiments.

Text S2

Characterizations. Characterization scanning electron microscopy (SEM, JSM-7500, JEOL, Japan), Raman spectroscopy (Raman, in Via, Renishaw Co., UK), Infrared spectroscopy (IR, Cary-600, Agilent, China), and X-ray diffraction (XRD, XD-6, General Instrumentation, Pukeno, China) were used to characterization of UiO-66 and PK/UiO-66. Energy dispersive spectroscopy (EDS, OXFORD Ultim Extreme, UK) was used to analyze the elemental distribution of the nanoparticles as well as the blades. Zeta potentials of all nanoparticles were obtained by dynamic scatterometry (Zetasizer Lab, Malvern Manalytical, UK).

Supplementary tables

Table S1. Particle size of different samples and PDI (n=3)

Sample	Average size / nm	PDI
UiO-66	72.86 ± 7.36	0.343 ± 0.057
PK/UiO-66	108.32 ± 12.47	0.447 ± 0.083

Table S2. The formulas and terms used in chlorophyll fluorescence determination.

Glossary of terms for O-J-I-P (PS II)	
PS II	Photosystem II
Q_A	Primary quinone acceptor of PS II
Q_B	Secondary quinone acceptor of PS II
RC	PS II reaction center
CS	Excited cross section
ABS	Absorption of solar flux
TR	Trapped energy flux
ET	Electron transport flux
DI	Dissipated energy flux
PI	Performance indexes
Fluorescence parameters derived from the extracted data	
$F_v \equiv F_t - F_0$	Variable fluorescence at time t
$F_m \equiv F_M - F_0$	Maximal variable fluorescence
Specific energy fluxes	
$ABS/RC = M_0(1/V_j)(1/\varphi_{P0})$	Absorption flux per RC
$TR_0/RC = M_0(1/V_j)$	Trapped energy flux per RC (at t = 0)
$ET_0/RC = M_0(1/V_j)\Psi_0$	Electron transport flux per RC (at t = 0)
$DI_0/RC = ABS/RC - TR_0/RC$	Dissipated energy flux per RC (at t = 0)
Yields or flux ratios	

$\varphi_{Po} = TR_0/ABS = [1 - (F_0/F_M)]$	Maximum quantum yield of primary photochemistry (at t = 0)
$\varphi_{P0} = ET_0/ABS = [1 - (F_0/F_M)]\varPsi_0$	Probability (at t = 0) that a trapped exciton moves an electron into the electron transport chain beyond QA-
$\varphi_{E0} = ET_0/ABS = [1 - (F_0/F_M)]\varPsi_0$	Quantum yield of electron transport (at t = 0)
$\varphi_{D0} = 1 - \varphi_{P0} = F_0/F_M$	Quantum yield of energy dissipation (at t = 0)

When $t=tFm$, CS was replaced by CSm.

Adapted from Strasser et al. (2004):

Strasser, R.J.; Tsimilli-Michael, M.; Srivastava, A. Analysis of the Chlorophyll a Fluorescence Transient. In: Papageorgiou, G.C., Govindjee (eds) Chlorophyll a Fluorescence. *Advances in Photosynthesis and Respiration*, 2004, 19, Springer, Dordrecht, DOI: 10.1007/978-1-4020-3218-9_12

Table S3. Normalized intensity ratios of UiO-66 peaks after PK coating.

2θ Range (°)	Peak Ratio	UiO-66	PK/UiO-66
5-8	I7.3°/I5.3°	1.00	0.79
25-30	I25.6°/I27.1°	1.00	0.83
30-40	I33.0°/I35.8°	1.00	0.86

Supplementary figures

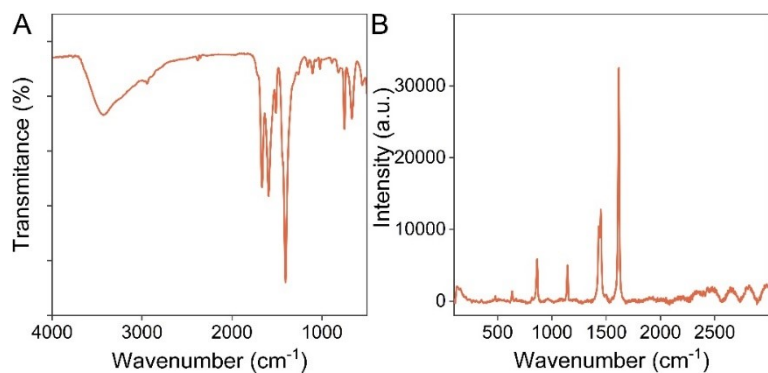


Fig. S1. IR (A) and Raman (B) spectrum of UiO-66.

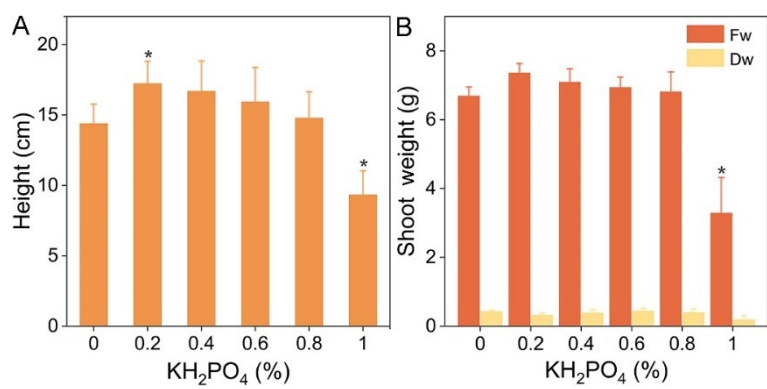


Fig. S2. Effects of different concentrations of KH_2PO_4 on pea growth. (A) Stem length; (B) Shoot weight.

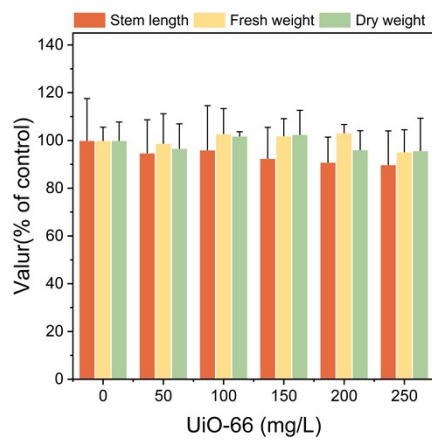


Fig. S3. Effect of UiO-66 spraying alone on pea growth.

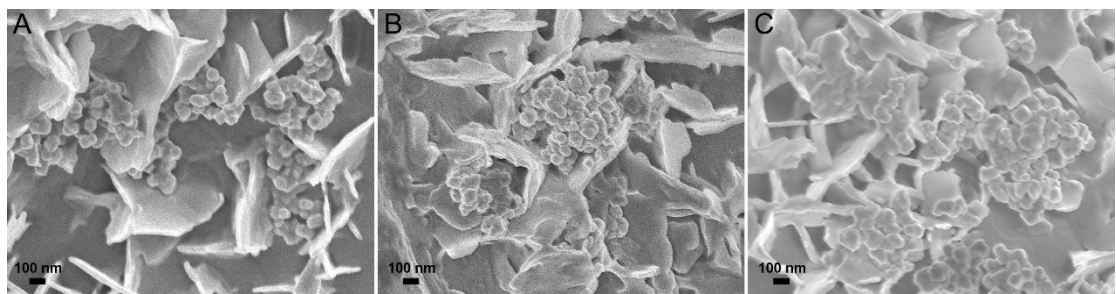


Fig. S4. Enlarged SEM image of the distribution of PK/UiO-66 NPs on the leaf surface.

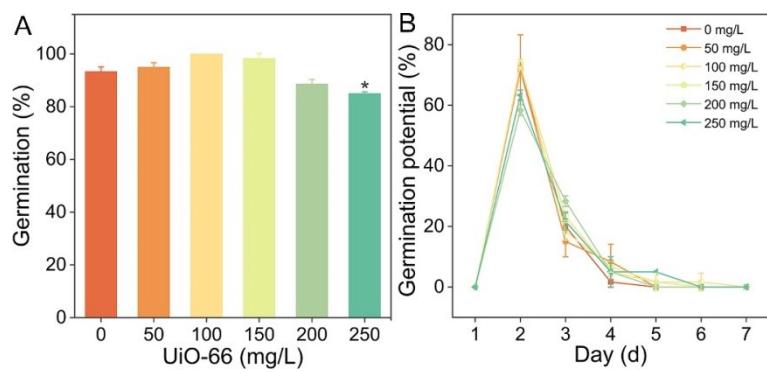


Fig. S5. Toxicity of UiO-66 to pea seeds. (A) Germination rate; (B) Germination potential.

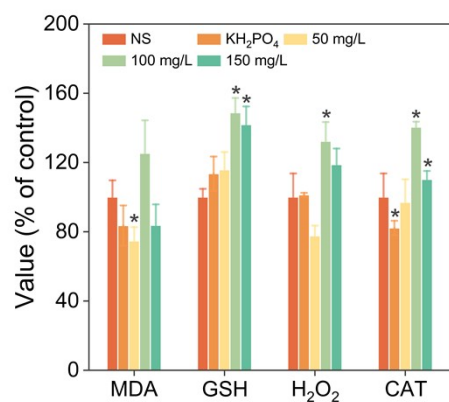


Fig. S6. Oxidative stress in pea leaves after foliar sprays.

Data availability

Data private access link: <https://www.scidb.cn/en/s/feAn2i>